Cogn Neurodyn (2007) 1:157–167
DOI 10.1007/s11571-006-9014-5

RESEARCH ARTICLE

Interaction between the Spatiotemporal Learning Rule (STLR) and Hebb type (HEBB) in single pyramidal cells in the hippocampal CA1 Area

Minoru Tsukada · Yoshiyuki Yamazaki · Hiroshi Kojima

Received: 29 June 2006 / Accepted: 18 October 2006 / Published online: 7 February 2007

Abstract The spatiotemporal learning rule (STLR), proposed as a non-Hebb type by Tsukada et al. (Neural Networks 9 (1996) 1357 and Tsukada and Pan (Biol. cyberm 92 (2005) 139), 2005), consists of two distinctive factors; ''cooperative plasticity without a cell spike,'' and ''its temporal summation''. On the other hand, Hebb (The organization of behavior. John Wiley, New York, 1949) proposed the idea (HEBB) that synaptic modification is strengthened only if the pre- and post-cell are activated simultaneously. We have shown, experimentally, that both STLR and HEBB coexist in single pyramidal cells of the hippocampal CA1 area. The functional differences between STLR and HEBB in dendrite (local)-soma (global) interactions in single pyramidal cells of CA1 and the possibility of pattern separation, pattern completion and reinforcement learning were discussed.

Keywords Spatiotemporal learning rule · Cooperative plasticity · Hebb learning rule · Dendrite–soma interaction · Hippocampus

Introduction

When we are confronted by certain situations, we naturally compare it to our previous experiences and attempt to predict what may happen. We then plan our actions in respect to those predicted outcomes that we found favorable. In this way, our past, present, and predictive (pre-future) memory act as one and determine our actions. Physiologically, it is believed that this contextual information is temporarily stored in the hippocampus. This hippocampal network consists of three types of synapses that form a circuit. A spatial-signal serves as the input to the hippocampus and is transmitted through a synapse in the dentate gyrus (DG) to the CA3, then through another synapse to the CA1. There also exists a simultaneous input, which directly connects to the CA1. The CA3 is also characterized by a distinct biological neural network, which has a recurrent (feedback) connection. This circuitry compiles past memory into the present. On this subject, Nakazawa et al. (2002) have reported that after knocking out feedback in the CA3 of mice using genetic techniques, an extremely large number of cues become required to accomplish one action. According to these observations, it can be hypothesized that the hippocampal CA3 network forms a context of time sequence, while the CA1 maps the spatiotemporal context into its synaptic weight space. For the CA3 $\rightarrow$ CA1 network, Tsuda (1996) and Tsuda and Kuroda (2001) proposed a computational model of chaos-driven contracting systems in which the unstable network (chaos-driven network, CA3) forms a context of events via chaotic itinerary and the stable network (contracting dynamics, CA1) encodes its information as Cantor coding. In the CA1, Tsukada et al. (1996), proposed STLR, which maps spatiotemporal information onto CA1 synaptic weight space. Tsukada and Pan (2005) showed that STLR had the highest efficiency in discriminating pattern sequences. The novel points of this learning rule were induction of cooperative plasticity without a postsynaptic spike and the time history

M. Tsukada (✉) · Y. Yamazaki · H. Kojima
Brain Science Center, Tamagawa University, 6-1-1, Tamagawagakuen, Machida, Tokyo 194-8610, Japan
e-mail: tsukada@eng.tamagawa.ac.jp

of its input sequences. On the other hand, Hebb (1949) proposed the idea that synaptic modification is strengthened only if the pre- and post-synaptic elements are activated simultaneously.

Experimentally, LTP and LTD are generally considered to be the cellular basis of learning. Recently, a series of experiments provided direct empirical evidence of Hebb's proposal. These reports indicated that synaptic modification can be induced by repetitive pairing of EPSP and back-propagating action potentials (BAPs) (Markram et al. 1997; Zhang et al. 1998; Feldman 2000; Boettiger and Doupe 2001; Sjostrom 2001; Froemke and Dan 2002). Pre-synaptic spiking within tens of milliseconds before postsynaptic spiking induced LTP whereas the reverse order resulted in LTD. This spike timing dependent LTP/LTD has been confirmed by using pyramidal cell pairs in hippocampal cultures (Debanne and Thompson 1998; Bi and Poo 1998), in which they found an asymmetric profile of LTP and LTD in relation to the relative timing between EPSPs and BAPs.

In this paper, we tested the following hypotheses on rat slice preparations by using an optical imaging method:

Experiment 1: The cooperative activity of input neurons can induce associative LTP (non-Hebb).
Experiment 2: Spike-timing dependent LTP (Hebb) also coexists in single cells.
Experiment 3: Non-Hebb LTP that is adopted as ''cooperative plasticity in STLR (non-Hebb) can be detected even in the absence of back propagating action potentials (BAPs) or output cell spikes by using an extra-cellular recording technique together with pharmacological treatments.

Finally, we discussed information-processing functions of dendrite (local)-soma (global) interactions in single cells based on the differences between STLR and HEBB.

Materials and methods

General methods

The experiments were performed on hippocampal slices, with a thickness of 400 μm, taken from female Wistar rats (4 weeks). The tissue was sliced at an angle of 30–45° to the long axis of the hippocampus. This angle was selected because the plane was parallel to the alvear fibers that were on the surface of the tissue and the trisynaptic circuit. The slices were maintained at 31°C in an experimental chamber with a normal medium, artificial cerebrospinal fluid (142 mM NaCl, 5.0 mM KCl, 2.6 mM NaH_2PO_4, 2.0 mM $MgSO_4$, 2.0 mM $CaCl_2$, 26 mM $NaHCO_3$, 10 mM glucose).

Experimental protocols

Experiment 1: Positions of the pair of stimulus electrodes are shown in Fig. 1A. Two bipolar tungsten electrodes (Stim.A and Stim.B) were placed at a fixed position in the stratum radiatum to stimulate the Schaffer collateral (SC) of CA3 (Fig. 1A). The optical recording area is depicted by a solid square (Fig. 1A) of which the left side was fixed at the boundary between the CA2 and CA1.

The intensity of the electric pulse to stimulate the SC (Stim.A and Stim.B) was fixed at a constant value. This was exactly half the intensity required to produce the maximum population in the CA1 region (0.1–0.5 mA). The duration of a stimulus pulse, total number of pulses and inter-stimulus interval (ISI) were fixed at 0.2 ms, 200 pulses and 2 s, respectively. The stimulus condition, Inter-stimulus interval (ISI) = 2 s,

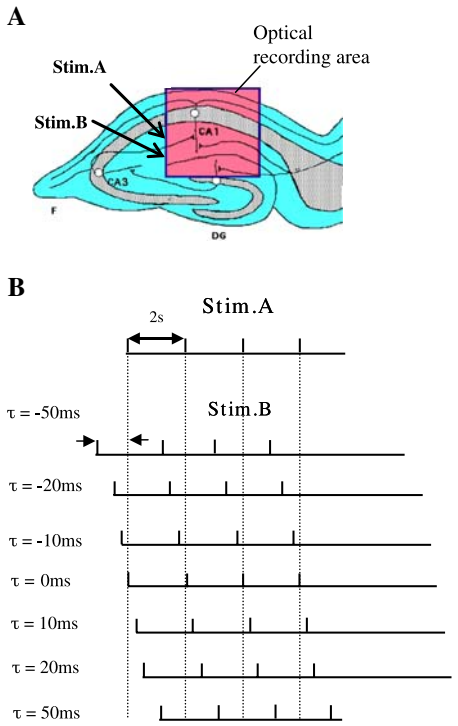

Fig. 1 Schematic drawing of Experiment 1. (**A**) Schematic representation of the hippocampal slice, showing the optical recording area (128 × 128 pixels, 1.75 mm × 1.75 mm) and the position of the two stimulating electrodes at a fixed position in the stratum radiatum of the CA1 area to stimulate the Schaffer collateral commissural of the CA3 region. (**B**) Schematic representation of the pairing stimulus pattern with spike timing (τ). The duration, total number, and inter-stimulus interval of stimulus pulses were fixed at 0.2 ms, 200 pulses, and 2 s, respectively

induced no LTP and LTD (Aihara et al. 1998). A pair of pulse stimuli (Stim.A and Stim.B) was used to stimulate the SC with various sets of relative timing ($\tau = t_B - t_A$), where the clock time of Stim.A (t_A) was a reference to that of Stim.B (t_B). The τ were 0, ±5, ±10, ±20, ±50 ms, seen in Fig. 1B.

Experiment 2: Positions of the pair of stimulus electrodes are shown in Fig. 2. One bipolar tungsten electrode was placed in stratum radiatum of the specific region to stimulate the SC of CA3 (Fig. 2, Stim.A). The other bipolar electrode was placed at a fixed position in the stratum oriens (Fig. 2, Stim.B). The optical recording area was depicted by a solid square (Fig. 2) of which the left side was fixed at the boundary between CA2 and CA1. The intensity of electric pulse to stimulate the SC (Stim.A) and SO (Stim.B) was fixed at a constant value. Exactly it was half intensity to produce the maximum population in CA1 region (0.1–0.5 mA). The duration of a stimulus pulse, total number of pulses and ISI were fixed at 0.2 ms, 200 pulses and 2 s, respectively. The stimulus condition, ISI = 2 s, induced no LTP or LTD (Aihara et al. 1998). A pair of pulse stimuli was used to stimulate the SC (Stim.A) and SO (Stim.B) with various sets of the relative timing ($\tau = t_B - t_A$), where the clock time of Stim.A (t_A) was a reference stimulus against that of Stim.B (t_B). The τ were 0, ±5, ±10, ±20, ±50 ms, seen in Fig. 1B.

Optical imaging

For optical imaging of Experiment 1–2, slices were stained for 40 min with 0.1 mg/ml RH482 in normal medium and were then washed and recovered for an additional 10 min. A naive slice was used for each stimulus sequence. Slices were viewed with 5 × objective. The voltage-sensitive dye signals were recorded with a 700 ± 30 nm interference filter. The transmitted light was detected by a 128 × 128 square array of photodiodes; each had a receptive area of 1.7 × 1.7 mm. Each photodiode received light from an area of 14 × 14 μm of the microscope objective field, and was coupled to current-to-voltage converter and amplifier (gain, 2000). We used the HR Deltaron 1700 system (Fujifilm microdevices Co.). This has an adequate resolution in space (14 × 14 μm/single photopixel) and in time (0.6 ms/single frame) to analyze spatio-temporal activities of the CA1 neural network. At the beginning of each experiment, the ''test stimulus'' (TS, at Stim.A site, single pulse) was applied once every 20 s (0.05 Hz) for more than 20 min to ensure that the amplitude of the population spike was stable. Thereafter, one of the paired stimuli with τ was delivered as a ''conditioning stimulus (CS).'' After giving the CS, the same TS was given every 20 s to estimate the change in responsiveness induced by CS. In the experiment, 16 responses were averaged to improve the signal to noise ratio for both unconditioned and conditioned (15–25 min after the CS) TS responses. The magnitude of LTP/LTD was estimated by mean percentage changes in the peak of 5 × 5 pixels in hippocampal CA1 slice (conditioned TS–response/unconditioned TS–response) (Fig. 3). A new slice was used for each stimulus sequence of TS/CS/TS. Seven slices were used for each paired stimulus. All values were expressed as the mean (%) ± standard error of the mean (SE); the results were evaluated statistically ($P < 0.05$) by analysis of variance (ANOVA).

Experiment 3: Glass recording microelectrodes were placed into the stratum radiatum of the CA1 region. Two independent bipolar microelectrodes were placed on either side of the recording electrode (within 150 μm from the recording electrode) (Fig. 4A). Responses were elicited by stimuli delivered alternatively to the two independent pathways through the respective isolation units at a frequency of 0.033 Hz to each pathway. Stimulus intensity versus response relationship was obtained for each slice at the beginning of experiments in order to determine the adequate stimulating intensity. The intensity (height) of the stimulating pulse (0.2 ms duration) was adjusted such that the initial slope of the extracellular field EPSPs (fEPSPs) was equal to 30–40% of the maximal value that was determined from the obtained intensity-response sigmoidal curve. The independence of each input was verified by demonstrating that the response evoked by each stimulating electrode was not affected by prior activation of the other. CA1 pyramidal cells

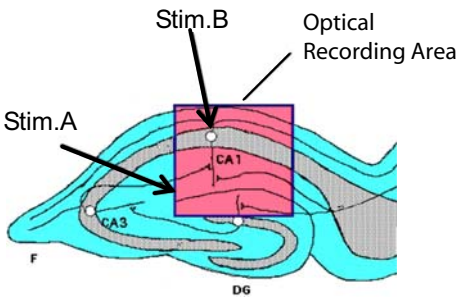

Fig. 2 Schematic drawing of Experiment 2. Schematic representation of the hippocampal slice showing stimulation and recording condition. Stim.A was placed at a fixed position in the stratum radiatum of the CA1 area to stimulate the Schaffer collateral commissural of the CA3 region. Stim.B was set on the stratum oriens bordering the alvelar, the output layer of the CA1, to initiate back-propagating action potentials. Also shows the optical recording area (128 × 128 pixels, 1.75 mm × 1.75 mm)

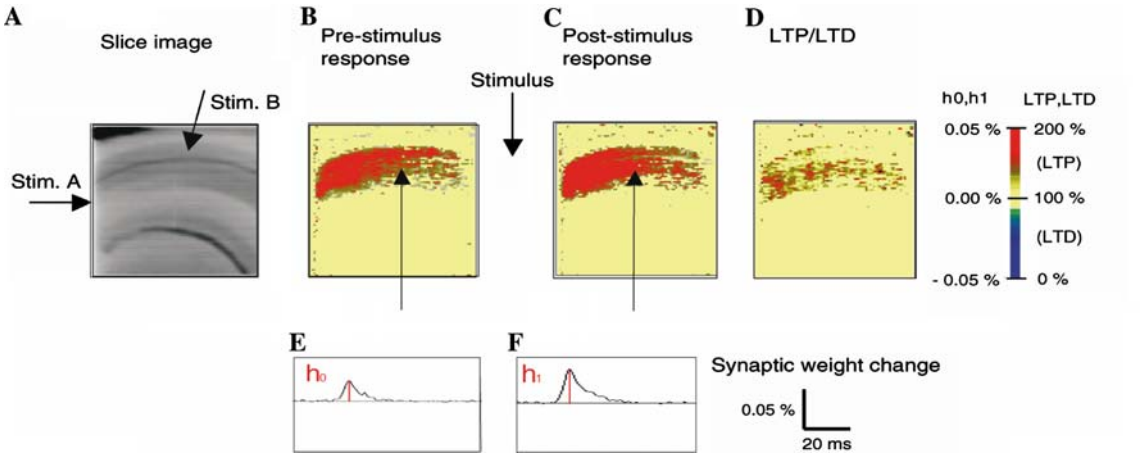

Fig. 3 Method of measuring LTP/LTD by optical imaging. (**A**) Image of the hippocampal CA1 area. (**B**) Spatial distribution of optical signals (fractional changes in light intensity) before a paired stimulus. (**C**) Spatial distribution of optical signals after a paired stimulus. (**D**) Spatial distribution of LTP/LTD plotted by the ratio (h_1/h_0) of the fractional changes in light intensity. (**E**, **F**) Optical signals h_0 and h_1 obtained by averaging 5×5 pixels at corresponding locations of before and after stimulus, respectively

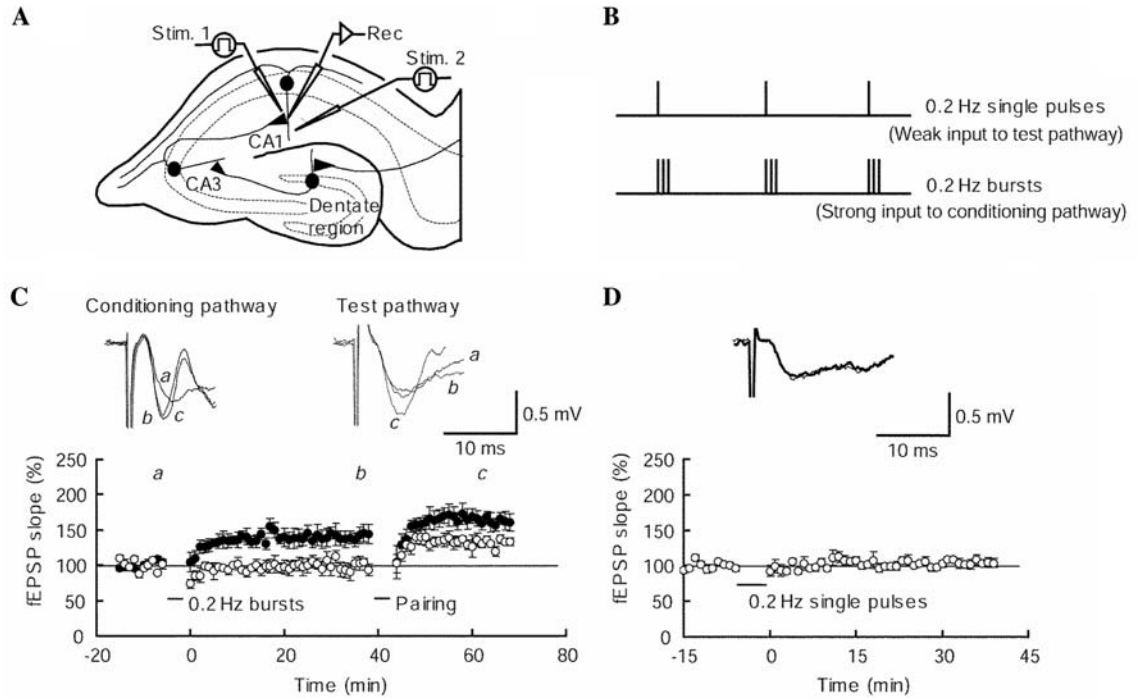

Fig. 4 Schematic drawing of Experiment 3. (**A**) Schematic representation of the hippocampal slice, showing the positioning of the two stimulating electrodes and the single recording electrode in the stratum radiatum of the CA1 region. (**B**) Schematic representation of the pairing stimulus. In the pairing protocol, 0.2 Hz single pulses were made to coincide with the first stimulus of 0.2 Hz bursts consisting of three pulses at 100 Hz (60 times, 5 min). (**C**) Demonstration of the properties of input-specificity and associativity in the induction of associative LTP. Top: Average of five typical traces of field excitatory postsynaptic potentials (fEPSPs) evoked in the conditioning and test pathways and collected at the times a–c indicated in the lower panel. All traces represented here were obtained from the same preparation. Bottom: Low-frequency stimulus-induced homo- and heterosynaptic LTP in the conditioning pathway (filled circles, with error bars indicating SEM) and test pathway (open circles) in hippocampal slices bathed in the normal ACSF ($n = 4$). (**D**) Demonstration of the properties of cooperativity. Top: Average of five typical traces of fEPSPs before (thin) and 35–40 min after (thick) the delivery of test pulses. Bottom: Test pulses alone did not alter the synaptic strength ($n = 6$)

were antidromically activated by using a stimulating electrode placed in the alveus and stimulation intensities sufficient to evoke near-maximal dendritic population spikes (recorded with an extracellular electrode in the stratum radiatum). Slices showing any evidence of contamination of the antidromic response by activation of fibers in the stratum oriens were not used.

Heterosynaptic associative LTP was induced by temporally pairing two trains of pulses (i.e., conditioning bursts to one pathway and test pulses to the other) by the following protocol: the conditioning bursts consisted of 60 trains of three pulses at 100 Hz, with an intertrain interval of 5 s; the test pulses, delivered in conjunction with each first pulse of the conditioning burst, therefore consisted of 60 pulses at 0.2 Hz (Huang et al. 2004; Fig. 4B). All data were shown as the mean ± SEM in the text, and Student's t-test or analysis of variance (ANOVA) was applied for statistical comparisons.

Pharmacological treatments

In Experiment 3, picrotoxin (20 μM) was present in the perfusion solution in order to suppress the $GABA_A$ receptor channels. The dendritic Na^+ channels were blocked by applying a low concentration of TTX (10–20 nM) to the perfusion solution and the final concentrations of TTX were achieved by mixing stock solutions with the perfusion solution.

Results

Associative LTP (Experiment 1)

The mapping of spatial information to synaptic space was measured by using two stimulus electrodes. First, electrode A was stimulated at 2 s intervals, but this did not produce any change in the synapse. Electrode B was then stimulated at a range of –50 to 50 ms in respect to electrode A. The relative timing between the two electrodes and the respective change measured in the synaptic weight of the hippocampus was then analyzed (Fig. 5). When the stimulus from both electrodes were simultaneous (relative timing $\tau = 0$), an extremely large plasticity appeared, but when it was shifted by 10 ms, there was almost no activity, and if it shifted another 10 ms, LTD appeared instead of LTP. When the relative timing was shifted 50 ms, it returned to normal. From these results, we learned that a time window exists in response to the relative timing, τ. That is, we observed the existence of a Mexican hat-shaped time window at the range of $\tau = \pm 50$ ms.

Spike timing dependent LTP/LTD (Experiment 2)

Figure 6 shows the optical imaging results of LTP and LTD induced by a series of different spike timing τ. The widest and strongest LTP was observed after simultaneous stimulation ($\tau = 0$ ms). LTP decreased rapidly in space and time as the absolute value of relative timing increased to 15 ms on both sides. Accordingly, LTP was induced when back propagating spikes (Stim.B) were applied within a time window of 15 ms before and after the onset of Stim.A, whereas LTD was induced on both sides at $|\tau| = 20$ ms. Outside the 50 ms time window, synaptic modification disappeared. From these results, LTP and LTD globally showed a symmetric window of spike timing similar to a ''Mexican hat function.''

Associative LTP independent of back propagated action potentials (BAPs) (Experiment 3)

We recorded the heterosynaptic associative LTP in the CA1 region, which was induced by a recently improved protocol applied to Schaffer collaterals (Huang et al. 2004), by measuring the initial slope of the fEPSPs as

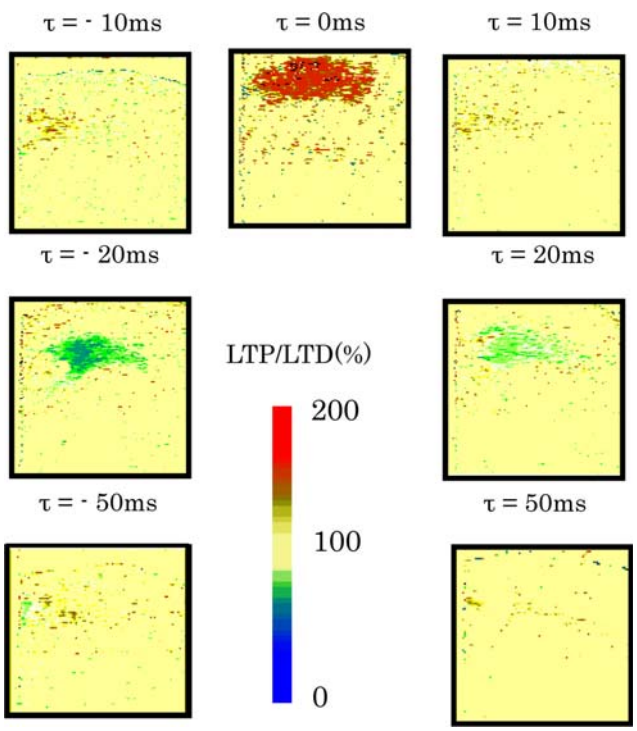

Fig. 5 Associative LTP/LTD by pairing stimulation. Spatial distribution of associative LTP and LTD in a naïve slice. The widest and strongest LTP was observed at $\tau = 0$ and the narrow and weak LTP at $\tau = \pm 10$ ms. Whereas LTD was induced at the value of $\tau = \pm 20$ ms. The profile LTP/LTD for τ globally showed a symmetric dependence

an index of synaptic efficacy. In general, LTP is classified into two main forms, (1) the heterosynaptic associative LTP that requires electrical activity both in the synapse at which LTP is observed and in one or more other synapses on the same neuron. This type of LTP requires electrical activity in two different synapses at once. (2) The homosynaptic LTP requires a tetanizing stimulus across the synapse at which LTP is observed. Robust homosynaptic LTP was produced by 60 conditioning bursts delivered to one afferent pathway (the conditioning pathway, strong input) for 5 min (Fig. 4C, filled circles; 144.2 ± 14.0% at 40 min after 0.2 Hz bursts; $n = 4$), whereas no transfer of the effect to the other pathway (the test pathway, weak input) was observed in the same slice preparation (Fig. 4C, open circles; 93.9 ± 8.2%) as long as the independency of the two pathways was preserved (see Methods).

After establishing stable homosynaptic LTP in the conditioning pathway, homo- and heterosynaptic LTP were induced at the potentiated conditioning pathway and test pathway, respectively, by further application of test pulses to the test pathway in temporal association with the conditioning bursts to the conditioning pathway (Fig. 4C; 169.4 ± 6.6 and 136.1 ± 5.0% in the conditioning and test pathways, respectively, at 20 min after pairing). The robust potentiation of the test pathway is a striking feature of the associative conditioning protocol, since the test pulses alone produced no change in the synaptic strength (Fig. 4D; 103.4 ± 6.0% at 40 min after 0.2 Hz single pulses; $n = 6$).

Effects of low TTX on amplitude of dendritic population spike but not on synaptic transmission

Optical recording experiments with a Ca^{2+} indicator have indicated that BAP-evoked Ca^{2+} transients were markedly reduced but reliable axonal conduction was preserved in CA1 pyramidal neurons in the presence of low TTX due to the lower safety factor for action potential propagation along the dendrite (Mackenzie and Murphy 1998). In order to test this possibility under our experimental conditions, we compared profiles of extracellular field potentials in the presence of low TTX (10–20 nM) between those evoked by stimulation of efferent pyramidal cell fibers in the alveus (antidromic) and those due to stimulation of afferent synaptic inputs in the stratum radiatum (Schaffer collaterals).

Figure 7A (left) illustrates a representative profile of extracellular field potentials recorded at the proximal stratum radiatum following suprathreshold alvear stimulation, which evoked a short-latency negative-going potential or ''dendritic population spike'' caused by action potentials which represent BAPs (Richardson et al. 1987). In agreement with an earlier observation (Miyakawa and Kato 1986), we observed that the amplitudes of BAPs were significantly reduced

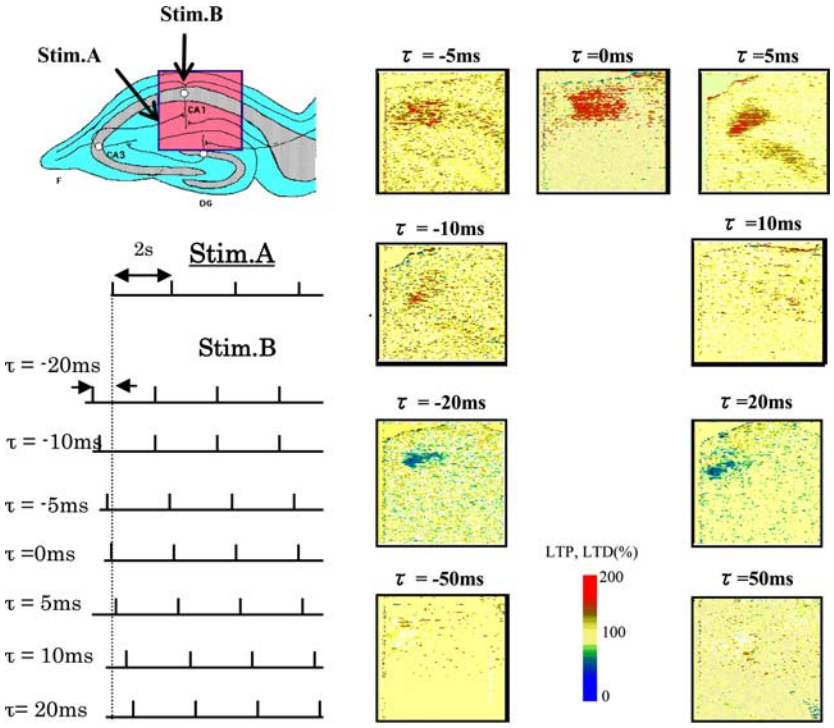

Fig. 6 Spatial distribution of spike timing dependent LTP (STDP) and LTD. The widest and strongest LTP was observed when simultaneous stimuli ($\tau = 0$) were applied. LTP decreased rapidly in space and time at $\tau = \pm 10$ ms. Whereas LTD was induced at $\tau = \pm 20$ ms, and if τ shifted ±50 ms, it return to normal

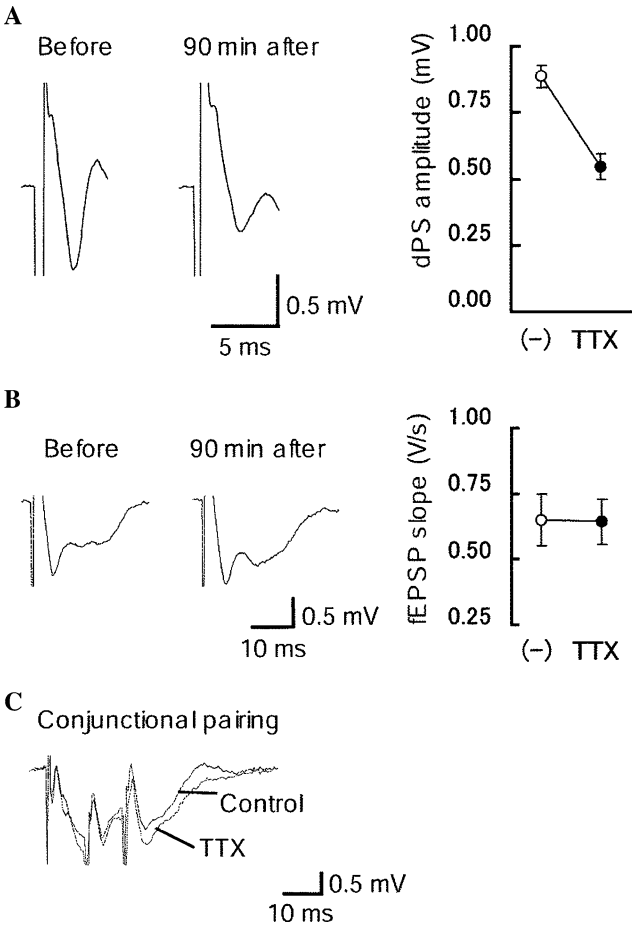

Fig. 7 Selective impairment of amplitude of dendritic population spike (dPS) but not slope of fEPSP by low TTX. (**A**) Low TTX-sensitivity of amplitude in dPS evoked by antidromic alvear stimulation. Left: Averaged profiles of dPS before and 90 min after bath-application of 10–20 nM TTX. Right: Significant reduction in the amplitude of dPS between before (–) and 90 min after (TTX) bath-application of 10–20 nM TTX. (**B**) Low TTX-insensitivity of basal synaptic transmission. Left: Averaged fEPSP traces before and 90 min after bath-application of 10–20 nM TTX. Right: No change in the slope of fEPSP between before (–) and 90 min after (TTX) bath-application of 10–20 nM TTX. (**C**) The complex EPSP response to conjunctional pairing of a test pulse and a conditioning burst was neither truncated nor reduced in terms of either duration or amplitude in the presence of low TTX

by bath-application of TTX (Fig. 7A; 0.89 ± 0.04 mV before vs. 0.55 ± 0.05 mV 90 min after low TTX bath application; $n = 4$; $P < 0.01$). In contrast, no significant change in the profile of fEPSPs evoked by stimulation of afferent synaptic inputs (Schaffer collaterals) during bath application of a similar concentration of TTX was observed (Fig. 7B; initial slope of fEPSP 0.65 ± 0.10 V s^{-1} before vs. 0.64 ± 0.09 V s^{-1} 90 min after the low TTX bath application; $n = 4$; $P > 0.9$). A small effect by BAPS still observed in Fig. 7B. However, it doesn't matter because the level of the effect is negligible. Therefore, consistent with the previous imaging experiments, the present results suggest that BAPs were markedly inhibited while the basal synaptic transmission remained unaffected in the presence of a low TTX.

Low TTX also had no significant effect on the profile of fEPSPs measured during a pairing stimulus protocol to induce associative LTP (Fig. 4C). This result suggests that the postsynaptic field response in the dendrite to conjunctive stimulation was contaminated by a small Na^+ channel-dependent component. Because it has been demonstrated that a blocker of N-methyl-D-aspartate (NMDA) receptors significantly truncated the profile of fEPSPs produced in response to a pairing protocol identical to that used in the present experiment, the fEPSP evoked during pairing stimulation is likely to consist dominantly of a NMDA-dependent component (Huang et al. 2004).

Low TTX reduced the magnitude of heterosynaptic associative LTP, but still a considerable amount of the LTP was preserved

It has been shown that only local dendritic depolarization at synaptic sites, such as theta-burst stimulation, could induce homosynaptic LTP even in the absence of BAP (Golding et al. 2002). In order to test whether conditioning bursts used in the present experiment could also induce homosynaptic LTP, we monitored the potentiation evoked in the conditioning pathway by application of the associative pairing protocols to Schaffer collaterals in the presence of low TTX. These pairing protocols were carried out after the observation of both the unchanged slope and reduced positive-going deflection of the fEPSP in the presence of low TTX, in order to make it conceivable that the low TTX actually inhibited BAPs (see previous section). As we expected, robust homosynaptically induced LTP was observed in both the absence and presence of low TTX in the conditioning pathway (Fig. 8A, C; (–), 155.5 ± 11.5%, $n = 11$; TTX, 142.6 ± 4.8%, $n = 9$; $P > 0.3$). These results suggest that homosynaptic LTP by the present pairing protocol was induced under the condition inhibiting activation of dendritic Na^+ channels and are consistent with a previous report that a brief application of TTX has no effect on the potentiation induced by high-frequency presynaptic stimulation (Thomas et al. 1998). However, in the same preparation, the magnitude of the heterosynaptically induced LTP in association with conditioning bursts was reduced, while a considerable amount of the LTP was preserved in the presence of low TTX (Fig. 8B, C; (–), 149.8 ± 9.6%; TTX, 122.1 ± 5.8%; $P < 0.05$).

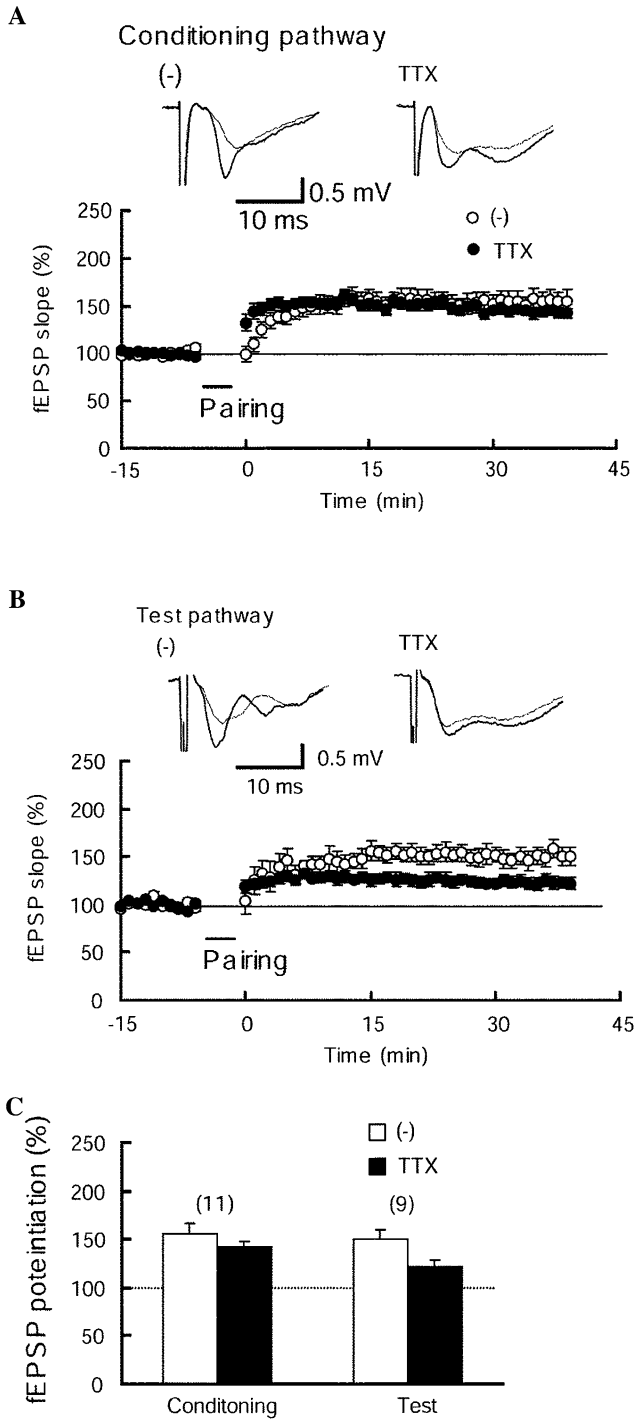

No significant difference in the magnitude of induced LTP between conditioning and test pathways ($P > 0.2$; paired t-test) was observed under the control condition, whereas that of the heterosynaptic LTP was significantly decreased compared with that of the homosynaptic LTP in the presence of low TTX ($P < 0.05$; paired t-test). These results suggest that Na^+ channel activation in the apical dendrites plays a significant role in the propagation of BAP.

◀ **Fig. 8** Low TTX-sensitivity in the induction of heterosynaptic associative LTP. (**A**, **B**) Effects of low TTX on low-frequency pairing-induced LTP in the conditioning (**A**) and test (**B**) pathway. Top: Averaged five typical traces of fEPSPs before (thin) and 35–40 min after (thick) the pairing in the absence (–) and presence (TTX) of 10–20 nM TTX. The pair of traces in conditioning and test pathway (represented in (**A**) and (**B**), respectively) was obtained from the same preparation under each condition. Bottom: Summarized low-frequency pairing-induced LTP in the control (open circles) and low TTX (filled circles) conditions. (**C**) Comparison of the effects of low TTX on the magnitude of LTP in the conditioning and test pathway at 40 min after pairing. The number of recorded slices for each group is shown in parentheses

Discussion

STLR (non-Hebb) and Hebb can coexist in the CA1 pyramidal cells of the Hippocampus

STLR (non-Hebb, Fig. 9) proposed by Tsukada et al. (1994, 1996, 2005) consisted of two defining factors; ''cooperative plasticity without a cell spike,'' and ''its temporal summation''. The two factors are preserved in a distributed way in the form of dendritic trees of a CA1 pyramidal cell, which should depend on the two classes of glutamate-receptor ion channel, NMDA and non-NMDA receptors co-localized at individual excitatory synapses. For the temporal summation, we have obtained evidence in neurophysiological experiments by applying temporal stimuli to schaffer collat-

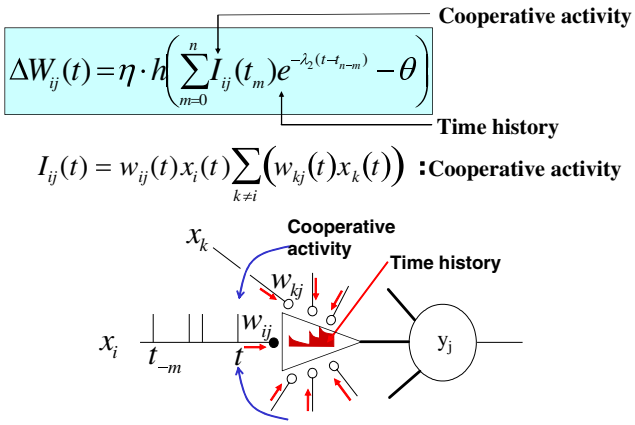

Fig. 9 The spatiotemporal learning rule (STLR). Where $w_{ij}(t)$; the value of a weight from neuron j to neuron i prior to adjustment, $\Delta w_{ij}(t) = w_{ij}(t + 1) - w_{ij}(t)$, η; the learning rate coefficient, $x_j(t)$; the level of excitation of input to neuron j, $y_i(t)$; the output of neuron I, $I_{ij}(t)$; the value of cooperative activity from neuron j to neuron i, $h(u)$; a sigmoid function of the potentiation force, θ is the thresholds, and λ_2 is the time decay constant of temporal summation which is a slow dynamic process ($\lambda_2 = 223$ ms) (Aihara et al. 2000)

erals of CA3 (Tsukada et al. 1994, 1996), while the cooperative plasticity without a cell spike has not been tested. In this paper, the coincidence of spike timing of Schafer collateral paired stimuli of CA3 played a crucial role in inducing associative LTP (cooperative plasticity) (Fig. 5). The homo-synaptic and hetero-synaptic associative LTP could be induced under conditions which inhibited BAPs (Fig. 8). Our results show that LTP can indeed occur at synapses on dendrites of hippocampal CA1 pyramidal cells, even in the absence of a cell spike. From these results, if the two inputs synchronize at the dendritic synapse of CA1 pyramidal cells, then the synapse is strengthened, and the functional connection is organized on the dendrite. If the two inputs are asynchronous then the connection is weakened. A schematic representation was drawn in Fig. 10. The functional connection/disconnection depends on the input–input timing dependent LTP (cooperative plasticity). This is different from the Hebbian learning rule, which requires coactivity of pre- and post-cell. STLR (non-Hebb) incorporated two dynamic processes; fast (10–30 ms) and slow (150–250 ms). The fast process works as a time window to detect a spatial coincidence among various inputs projected to a weight space of the hippocampal CA1 dendrites, while the slow process works as a temporal integrator of a sequence of events. In a previous paper (Aihara et al. 2000), by parameter fitting to the physiological data of LTPs time scale, the decay constant of fast dynamics was identified as 17 ms, which matches the period of hippocampal gamma oscillation. The decay constant of the slow is 169 ms, which corresponds to a theta rhythm. This suggests that cell assemblies are synchronized at two time scales in the hippocampal-cortical memory system and is closely related to the memory formation of spatio-temporal context.

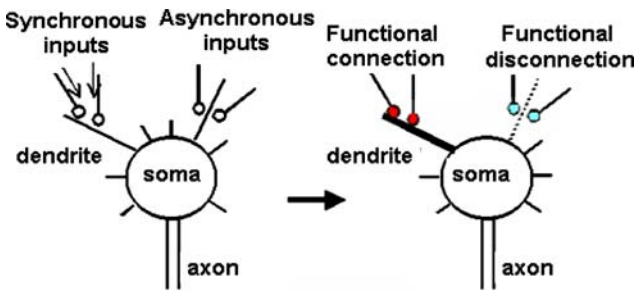

Fig. 10 A schematic representation of functional connection/disconnection, depending on cooperative activity dependent LTP/LTD

On the other hand, Hebbian learning is characterized by coincident pre- and post-cell activity; the interconnected weights which contribute to fire a post-cell are strengthened according to the delta rule. Supporting this point of view, a series of experiments have shown that synaptic modification can be induced by repetitive pairing of EPSPs and BAPs, providing direct empirical evidence to support Hebb's proposal (Markram et al. 1997; Magee and Johnston 1997; Zhang et al. 1998; Debanne et al. 1998; Bi and Poo 1998; Feldman 2000; Boettiger and Doupe 2001; Sjostrom et al. 2001; Froemke and Dan 2002). In this paper, spike timing dependent LTP was induced in the CA1 area of a hippocampal slice using optical imaging when back propagating spikes (Stim.B) were applied within a time window of 15 ms before and after the onset of Stim.A (Schaffer-commissural collateral of CA3). The heterosynaptically induced LTP in association with conditioning bursts was significantly reduced in the presence of low TTX (Fig. 8B, C).

From these experimental results, it is concluded that two learning rules, STLR and HEBB, must coexist in single pyramidal neurons of the hippocampal CA1 area.

The functional differences between STLR and HEBB

We applied two rules to a single-layered neural network and compared its ability of separating spatio-temporal patterns with that of other rules, including the Hebbian learning rule and its extended rules. The simulated results (Tsukada and Pan 2005) showed that STLR (non-Hebb) has the highest efficiency in discriminating spatiotemporal pattern. On the other hand HEBB has a natural tendency to attract analogous firing patterns into a representative one, in the simple word ''pattern completion'' (Guzowski et al. 2004). From this it is concluded that STLR has a high ability in pattern separation, while HEBB has a high ability in pattern completion.

We also expand upon the results from theoretical simulation to imply a phenomenon occurring in a dendrites-soma system in single pyramidal cells with many independent local dendrites in the CA1 area of the hippocampus. This system includes a spine structure, NMDA receptors (NMDAR), and Sodium and Calcium channels. The pyramidal cell integrates all of these local dendrite functions.

A schematic illustrations were drawn in Fig. 11A, B. HEBB leads to the pattern completion (Fig. 11A). In contrast, STLR leads to the pattern separation (Fig. 11B).

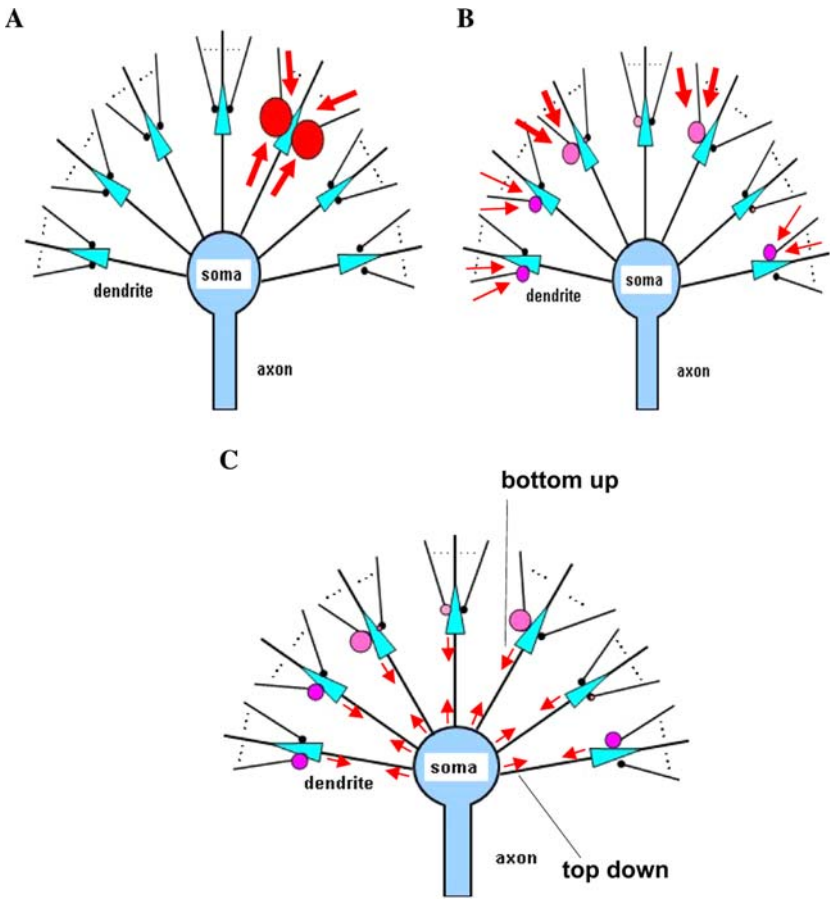

Fig. 11 Functional differences between Hebb (**A**), and STLR (**B**), and their interaction in a dendrite (local)–soma (global) system of single pyramidal cells of the CA1

Dendrite (local)–soma (global) interactions in single pyramidal cells of CA1

From these results, it was revealed that STLR and HEBB coexist in single pyramidal neurons of the hippocampal CA1 area. In STLR, synaptic weight changes are determined by the ''synchrony'' level of input neurons and its temporal summation (bottom-up), while in HEBB, the soma fires by integrating dendritic local potentials or by top-down information such as environmental sensitivity, awareness, consciousness (top-down) (Fig. 11C).

The role of soma spiking as top-down information raise a number of interesting computational predictions. Hippocampal theta is one of candidates of top-down information which is driven by medial septum (Buzsaki et al. 1983; Stewart and Fox et al. 1990). The theta stimulation of adult rat hippocampal synapses can induce LTP (Thomas et al. 1998). Second is extrinsic modulators such as acetylcholine, serotonin, norepinephrine and dopamine. They can alter neuronal throughput and BAPs (so-called ''meta-plasticity'') in such way that these transmitters diffuse broadly (Tsubokawa and Ross 1997; Sandra and Ross 1999; Pitler and Alger 1992).

When we are confronted by certain situations, we naturally compare it to our previous experiences and attempt to predict what may happen and plan our actions in respect to those predicted outcomes that we found favorable. In this way, our past, present, and prefuture memory act as one and determine our actions. If these actions do not fit, then a new hypothesis is formulated, new data is reasoned, and the previous model is amended. The coexistence of STLR and HEBB may support this dynamic process, which repeats itself until the internal model fits the outer environment. In reinforcement learning, the dendritic–soma interaction in single pyramidal neurons of the hippocampal CA1 area can play an important role in the context formation of policy, reward, and value.

Acknowledgements This study was supported by The 21st Century Center of Excellence Program (Integrative Human Science Program, Tamagawa Univ.) and by a Grant-in-Aid for Scientific Research on Priority Areas—Integrative Brain Science Project—from the Ministry of Education, Culture, Sports, Science nd Technology, Japan.

References

Aihara T, Kobayashi Y, Matsuda H, Sasaki H, Tsukada M (1998) Optical imajing of LTP and LTD induced simultaneously by temporal stimulus in hippocampal CA1 area. Soc Neurosci Abs 24:1070

Aihara T, Tsukada M, Matsda H (2000) Two dynamic processes for the induction of long-term in hippocampal CA1 neurons. Biol Cybern 82:189–195

Bi G, Poo M (1998) Synaptic modifications in cultured hippocampal neurons; dependence on spike timing, synaptic strength, and postsynaptic type. J Neurosci 18:10464–10472

Boettiger CA, Doupe AJ (2001) Developmentally restricted synaptic plasticity in a songbird nucleus required for song learning. Neuron 31:809–818

Buzsaki G, Leung L, Vanderwolf CH (1983) Celluler bases of hippocampal EEG in the behaving rat. Brain Res Rev 6:169–171

Debanne D, Thompson SM (1998) Associative long-term depression in the hippocampus in vitro. Hippocampus 6:9–16

Feldman DE (2000) Timing based LTP and LTD at vertical inputs to layer II/III pyramidal cells in rat barrel cortex. Neuron 27:45–56

Froemke RC, Dan Y (2002) Spike-timing-dependent synaptic modification induced by natural spike trains. Nature 416:433–438

Golding NL, Staff NP, Spruston N (2002) Dendritic spikes as a mechanism for cooperative long-term potentiation. Nature 418(6895):326–331

Guzowski JF, Knierim JJ, Moser EI (2004) Ensemble dynamics of hippocampal regions CA3 and CA1. Neuron 44:581–584

Hebb DO (1949) The organization of behavior. New York, John Wiley

Huang YY, Pittenger C, Kandel ER (2004) A form of long-lasting, learning-related synaptic plasticity in the hippocampus induced by heterosynaptic low-frequency pairing. Proc Natl Acad Sci USA 101(3):859–864

Mackenzie PJ, Murphy TH (1998) High safety factor for action potential conduction along axons but not dendrites of cultured hippocampal and cortical neurons. J Neurophysiol 80(4):2089–2101

Magee JC, Johnston D (1997) A synaptically controlled, associative signal for Hebbian plasticity in hippocampal neurons. Science 275(5297):209–213

Markram H, Lubke J, Frotscher M, Sakmann B (1997) Reguration of synaptic efficacy by coincidence of postsynaptic Aps and EPSPs. Science 275:213–215

Miyakawa H, Kato H (1986) Active properties of dendritic membrane examined by current sourcedensity analysis in hippocampal CA1 pyramidal neurons. Brain Res 399(2):303–309

Nakazawa K, Quirk MC, Chitwood RA, Watanabe M, Yeckel MF, Sun LD, Kato A, Carr CA, Johnston D, Wilson MA, Tonegawa S (2002) Requirement for hippocampal CA3 NMDA recepters in associative memory recall. Science 297:211–218

Pitler TA, Alger BE (1992) Postsynaptic spike firing reduces synaptic $GABA_A$ responses in hippocampal pyramidal cells. J Neurosci 12:4122–4132

Richardson TL, Turner RW, Miller JJ (1987) Action potential discharge in hippocampal CA1 pyramidal neurons: current source density analysis. J Neurophysiol 58(5): 981–996

Sandler VM, Ross WM (1999) Serotonin modulated spike back-propagation and associated $[Ca^{2+}]$ changes in apical dendrites of hippocampal CA1 pyramidal neurons. J Neurophysiol 81:216–224

Sjostrome PJ (2001) Rate timing, and cooperativity jointly determine cortical synaptic plasticity. Neuron 32:1149–1164

Stewart M, Fox SE (1990) Do septum neurons pace the hippocampal theta rhythm? Trends Neurosci 13:163–168

Thomas MJ, Watabe AM, Moody TD, Makhinson M, O'Dell TJ (1998) Postsynaptic complex spike bursting enables the induction of LTP by theta frequency synaptic stimulation. J Neurosci 18(18):7118–7126

Tsubokawa H, Ross WM (1997) Muscarinic modulation of spike back-propagation in the apical dendrites of hippocampal CA1 pyramidal neurons. J Neurosci 17:5782–5791

Tsuda I (1996) A New type of self-organization associated with chaotic dynamics in neural networks. Int J Neural Sys 7:451–459

Tsuda I, Kuroda S (2001) Cantor coding in the hippocampus. Jpn J Indust Appl Math 18:249–258

Tsukada M, Aihara T, Mizuro M, Kato H, Ito K (1994) Temporal pattern sensitivity of long-term potentiation in hippocampal CA1 neurons. Biol Cybern 70:495–503

Tsukada M, Aihara T, Saito H, Kato H (1996) Hippocampal LTP depends on spatial and temporal correlation of inputs. Neural Networks 9:1357–1365

Tsukada M, Pan X (2005) The spatiotemporal learning rule and its efficiency in separating spatiotemporal patterns. Biol Cybern 92:139–146

Zhang LI, Tao HW, Holt CE, Harris WA, Poo M (1998) A critical window for cooperation and competition among developing retino-tectal synapses. Nature 395:37–44